Aquatic laser fluorescence analyzer: field evaluation in the northern Gulf of Mexico

Alexander Chekalyuk,[1,*] Andrew Barnard,[2] Antonietta Quigg,[3,4] Mark Hafez,[1] and Yan Zhao[4]

[1]*Lamont Doherty Earth Observatory of Columbia University, 61 Route 9W, Palisades, New York 10964, USA*
[2]*WET Labs, Inc., PO Box 518, Philomath, Oregon 97370, USA*
[3]*Department of Marine Biology, Texas A&M University, Galveston campus, 200 Seawolf Parkway, Galveston, Texas 77553 USA*
[4]*Department of Oceanography, Texas A&M University, 3146 TAMU, College Station, Texas 77843 USA*
[*]*chekaluk@ldeo.columbia.edu*

Abstract: The new Aquatic Laser Fluorescence Analyzer (ALFA) provides spectral and temporal measurements of laser-stimulated emission (LSE) for assessment of phytoplankton pigments, community structure, photochemical efficiency (PY), and chromophoric dissolved organic matter (CDOM). The instrument was deployed in the Northern Gulf of Mexico to evaluate the ALFA analytical capabilities across the estuarine-marine gradient. The robust relationships between the pigment fluorescence and independent pigment measurements were used to validate the ALFA analytical algorithms and calibrate the instrument. The maximal PY magnitudes, $PY_m = PY(1\text{-}1.35\cdot10^{-4}PAR)^{-1}$, were estimated using the underway measurements of PY and photosynthetically active radiation (PAR). The chlorophyll (Chl) spatial patterns were calculated using the ratio of Chl fluorescence to PY to eliminate the effect of non-photochemical quenching on the underway Chl assessments. These measurements have provided rich information about spatial distributions of Chl, PY_m, CDOM, and phytoplankton community structure, and demonstrated the utility of the ALFA instrument for oceanographic studies and bio-environmental surveys. The data suggest that the fluorescence measurements with 514 nm excitation can provide informative data for characterization of the CDOM-rich fresh, estuarine, and coastal aquatic environments.

OCIS codes: (010.4450) Oceanic optics; (280.4788) Optical sensing and sensors; (300.0300) Spectroscopy; (140.0140) Lasers and laser optics.

References and links

1. A. M. Chekalyuk and M. Hafez, "Advanced laser fluorometry of natural aquatic environments," Limnol. Oceanogr. Methods **6**, 591–609 (2008).
2. A. M. Chekalyuk and M. Hafez, "Photo-physiological variability in phytoplankton chlorophyll fluorescence and assessment of chlorophyll concentration," Opt. Express **19**(23), 22643–22658 (2011).
3. A. M. Chekalyuk, M. Landry, R. Goericke, A. G. Taylor, and M. Hafez, "Laser fluorescence analysis of phytoplankton across a frontal zone in the California Current ecosystem," J. Plankton Res. **34**(9), 761–777 (2012).
4. A. M. Chekalyuk and M. A. Hafez, "Next generation Advanced Laser Fluorometry (ALF) for characterization of natural aquatic environments: new instruments," Opt. Express **21**(12), 14181–14201 (2013).
5. D. Marie, F. Partensky, S. Jacquet, and D. Vaulot, "Enumeration and cell cycle analysis of natural populations of marine picoplankton by flow cytometry using the nucleic acid stain SYBR Green I," Appl. Environ. Microbiol. **63**(1), 186–193 (1997).
6. A. S. McInnes, A. K. Shepard, E. J. Raes, A. M. Waite, and A. Quigg, "Carbon and Nitrogen Fixation: Simultaneous quantification of active communities and estimation of rates using Fluorescence in situ Hybridization and Flow Cytometry," Appl. Environ. Microbiol. (submitted).
7. M. D. Ohman, D. L. Rudnick, A. Chekalyuk, R. E. Davis, R. A. Feely, M. Kahru, H.-J. Kim, M. R. Landry, T. R. Martz, C. L. Sabine, and U. Send, "Autonomous ocean measurements in the California Current Ecosystem,"

#214306 - $15.00 USD Received 18 Jun 2014; revised 15 Aug 2014; accepted 15 Aug 2014; published 29 Aug 2014

Oceanography (Wash. D.C.) **26**(3), 18–25 (2013).
8. J. I. Goes, H. R. Gomes, A. M. Chekalyuk, E. J. Carpenter, J. P. Montoya, V. J. Coles, P. L. Yager, W. M. Berelson, D. G. Capone, R. A. Foster, D. K. Steinberg, A. Subramaniam, and M. A. Hafez, "Influence of Amazon River discharge on the biogeography of phytoplankton communities in the western tropical north Atlantic," Prog. Oceanogr. **120**, 29–40 (2014), doi:10.1016/j.pocean.2013.07.010.
9. J. I. Goes, H. R. Gomes, E. M. Haugen, K. T. McKee, E. J. D'Sa, A. M. Chekalyuk, D. K. Stoecker, P. J. Stabeno, S.-I. Saitoh, and R. N. Sambrotto, "Fluorescence, pigment, and microscope characterization of Bering Sea phytoplankton community structure and photosynthetic competency in the presence of a Cold Pool during summer," http://www.sciencedirect.com/science/article/pii/S0967064513004505
10. A. M. Chekalyuk, "Optical analysis of emissions from stimulated liquids," Patent application WO2013116769 A1 (2013).
https://www.google.com/patents/WO2013116760A1?cl=en&dq=WO2013116760+A1&hl=en&sa=X&ei=N9FKUsJ4863gA8n8gcgB&ved=0CDkQ6AEwAA
11. A. M. Chekalyuk and M. Hafez, "Analysis of spectral excitation for measurements of fluorescence constituents in natural waters," Opt. Express **21**(24), 29255–29268 (2013).
12. A. Barnard, A. M. Chekalyuk, A. Derr, W. Strubhar, M. A. Hafez, J. Pearson, C. Orrico, and C. Moore, "Aquatic Laser Fluorescence Analyzer (ALFA): A new instrument for characterization of natural aquatic environments," AGU 2012 Ocean Sciences Meeting (2012).
http://www.sgmeet.com/osm2012/viewabstract2.asp?AbstractID=11217.; see also
http://www.wetlabs.com/aquatic-laser-fluorescence-analyzer-alfa.
13. R. E. Turner and N. N. Rabalais, "Coastal eutrophication near the Mississippi River delta," Nature **368**(6472), 619–621 (1994).
14. N. N. Rabalais, W. J. Wiseman, R. E. Turner, D. Justić, B. K. Gupta, and Q. Dortch, "Nutrient changes in the Mississippi River and system responses on the adjacent continental shelf," Estuaries **19**(2), 386–407 (1996).
15. R. E. Turner and N. N. Rabalais, "Nitrogen and phosphorus phytoplankton growth limitation in the northern Gulf of Mexico," Aquat. Microb. Ecol. **68**(2), 159–169 (2013).
16. J. B. Sylvan, A. Quigg, S. Tozzi, and J. W. Ammerman, "Eutrophication-induced phosphorus limitation in the Mississippi River plume: evidence from fast repetition rate fluorometry," Limnol. Oceanogr. **52**(6), 2679–2685 (2007).
17. J. B. Sylvan, A. Quigg, S. Tozzi, and J. W. Ammerman, "Mapping phytoplankton community physiology on a river impacted continental shelf: testing a multifaceted approach," Estuaries Coasts **34**(6), 1220–1233 (2011).
18. A. Quigg, J. B. Sylvan, A. B. Gustafson, T. R. Fisher, R. L. Oliver, S. Tozzi, and J. W. Ammerman, "Going west: nutrient limitation of primary production in the Northern Gulf of Mexico and the importance of the Atchafalaya River," Aquat. Geochem. **17**(4-5), 519–544 (2011).
19. Y. Zhao and A. Quigg, "Nutrient limitation in Northern Gulf of Mexico (NGOM): phytoplankton communities and photosynthesis respond to nutrient pulse," PLoS ONE **9**(2), e88732 (2014), doi:10.1371/journal.pone.0088732.
20. Y. R. Qian, A. E. Jochens, M. C. Kennicutt II, and D. C. Biggs, "Spatial and temporal variability of phytoplankton biomass and community structure over the continental margin of the northeast Gulf of Mexico based on pigment analysis," Cont. Shelf Res. **23**(1), 1–17 (2003).
21. B. A. Schaeffer, J. C. Kurtz, and M. K. Hein, "Phytoplankton community composition in nearshore coastal waters of Louisiana," Mar. Pollut. Bull. **64**(8), 1705–1712 (2012).
22. R. J. Olson, A. M. Chekalyuk, and H. M. Sosik, "Phytoplankton photosynthetic characteristics from fluorescence induction assays of individual cells," Limnol. Oceanogr. **41**(6), 1253–1263 (1996).
23. D. N. Klyshko and V. V. Fadeev, "Remote determination of concentration of impurities in water by the laser spectroscopy method with calibration by Raman scattering," Sov. Phys. Dokl. **23**, 55–59 (1978).
24. F. E. Hoge and R. N. Swift, "Airborne simultaneous spectroscopic detection of laser-induced water Raman backscatter and fluorescence from chlorophyll a and other naturally occurring pigments," Appl. Opt. **20**(18), 3197–3205 (1981).
25. R. J. Exton, W. M. Houghton, W. E. Esaias, R. C. Harriss, F. H. Farmer, and H. H. White, "Laboratory analysis of techniques for remote sensing of estuarine parameters using laser excitation," Appl. Opt. **22**(1), 54–64 (1983).
26. T. J. Cowles, R. A. Desiderio, and S. Neuer, "In situ characterization of phytoplankton from vertical profiles of fluorescence emission spectra," Mar. Biol. **115**(2), 217–222 (1993).
27. M. Vernet, B. G. Mitchell, and O. Holm-Hansen, "Adaptation of Synechococcus in situ determined by variability in intracellular phycoerythrin-543 at a coastal station off the Southern California coast, USA," Mar. Ecol. Prog. Ser. **63**, 9–16 (1990).
28. A. Bricaud, M. Babin, A. Morel, and H. Claustre, "Variability in the chlorophyll-specific absorption coefficients of natural phytoplankton: Analysis and parameterization," J. Geophys. Res. **100**(C7), 13321–13332 (1995).
29. R. Williams and H. Claustre, "Photosynthetic pigments as biomarkers oof phytoplankton populations and processes involved in the transformation of particulate organic matter at the Biotrans site (47°N, 20°W)," Deep-Sea Res. Part A, Oceanograph. Res. Papers **38**, 347–355 (1991).
30. D. M. Kehoe and A. Gutu, "Responding to color: the regulation of complementary chromatic adaptation," Annu. Rev. Plant Biol. **57**(1), 127–150 (2006).
31. B. Palenik, "Chromatic adaptation in marine *Synechococcus* strains," Appl. Environ. Microbiol. **67**(2), 991–994 (2001).

#214306 - $15.00 USD Received 18 Jun 2014; revised 15 Aug 2014; accepted 15 Aug 2014; published 29 Aug 2014

32. A. M. Chekalyuk, F. E. Hoge, C. W. Wright, R. N. Swift, and J. K. Yungel, "Airborne test of laser pump-and-probe technique for assessment of phytoplankton photochemical characteristics," Photosynth. Res. **66**(1-2), 45–56 (2000).
33. P. G. Falkowski and Z. Kolber, "Variations in chlorophyll fluorescence yields in phytoplankton in the world oceans," Aust. J. Plant Physiol. **22**(2), 341–355 (1995).
34. Z. S. Kolber, O. Prasil, and P. G. Falkowski, "Measurements of variable chlorophyll fluorescence using fast repetition rate techniques: Defining methodology and experimental protocols," Biochem. Biophys. Acta **1367**(1-3), 88–106 (1998).

1. Introduction

The Advanced Laser Fluorometry (ALF; see the Table of Abbreviations in Appendix [Table 1]) [1] is an analytical technique that addresses the optical complexity of natural aquatic environments to characterize the key fluorescence constituents (phytoplankton pigments, biomass, photophysiology, phycobiliprotein (PBP) containing phytoplankton groups, and CDOM). The original ALF fluorometer is a compact flow-through instrument that combines spectral and temporal LSE measurements using dual-wavelength excitation at 405 and 532 nm. It is used for underway shipboard measurements and analysis of discrete water samples [1–3]. The spectral deconvolution (SDC) analysis of the LSE signatures is used to assess the overlapped spectral bands of aquatic fluorescence constituents. Along with the accurate concentration measurements, the SDC provides quantification of the non-chlorophyll fluorescence background in the spectral area of Chl fluorescence for more accurate assessments of phytoplankton photo-physiological parameter, PY [1,4]. The ALF measurements of variable fluorescence can be used to improve assessments of Chl concentration [2].

The major ALF advantages over other techniques capable of phytoplankton structural characterization are that it provides additional useful information about phytoplankton photo-physiology and CDOM, conducts the measurements directly in the sampled water without any preparation and treatment of the sample, can be used for fast automatic real-time analysis in various settings, including high-resolution underway measurements from small vessels and motorboats [1]. On the other hand, the ALF capacity for phytoplankton structural characterization is limited to assessment of the PBP-containing cyanobacteria and cryptophytes, while other techniques used in the oceanography, such as flow cytometry or DNA analysis, can provide more detailed information on phytoplankton community structure and size distributions (e.g., [5]), as well as activity and functional roles of the dominant species (e.g., [6]).

In 2006-2011, the ALF technique was extensively tested in diverse water types (including Chesapeake and Delaware Bays, the California Current, Bering Sea, Gulf of Mexico, and the Amazon River Plume) and proved to be a useful tool for aquatic research and environmental monitoring. It was used for assessment of Chl concentration, phytoplankton biomass and photochemical efficiency (PY), detection and quantification of PBP-containing cyanobacteria and cryptophytes, and measurements of CDOM spatial variability [1–3, 7–9].

These field deployments provided useful information to identify the ALF design solutions and analytical algorithms that needs to be further refined. The new instrument components, including miniature spectrometers and lasers with new emission wavelengths, have become available. These factors facilitated development of the next generation ALF technology. Several new options for the optical design and ALF instrument configuration were developed [10]. A single-laser (514 nm) and three-laser ALF-T instruments comprising new 514 and 375 nm lasers were built and tested in the laboratory and field conditions [4]. These and earlier ALF measurements were analyzed to optimize the spectral excitation for operation in various water types [11].

A new commercial instrument, the Aquatic Laser Fluorescence Analyzer [12] (ALFA), has been recently developed on this basis in collaboration between the Lamont-Doherty Earth Observatory of Columbia University and Western Environmental Technology Laboratories,

#214306 - $15.00 USD Received 18 Jun 2014; revised 15 Aug 2014; accepted 15 Aug 2014; published 29 Aug 2014

Inc. (WET Labs). The benchtop ALFA instrument operationally implements the key design solutions, measurement protocols and analytical methods of the ALF technique. It provides spectrally and temporally resolved LSE measurements for assessment of phytoplankton pigment biomass, PBP-containing phytoplankton groups, PY, and CDOM. It can be used for laboratory and field flow-through measurements with an external water supply, and for analysis of water samples using a miniature peristaltic pump installed on the front panel of the instrument case [Fig. 1]. In the dual-laser instrument configuration, ALFA-405/514, the alternate laser excitation at 405 and 514 nm is used for characterization of the fluorescence constituents in a broad range of water types, including fresh, estuarine, coastal and offshore waters [11].

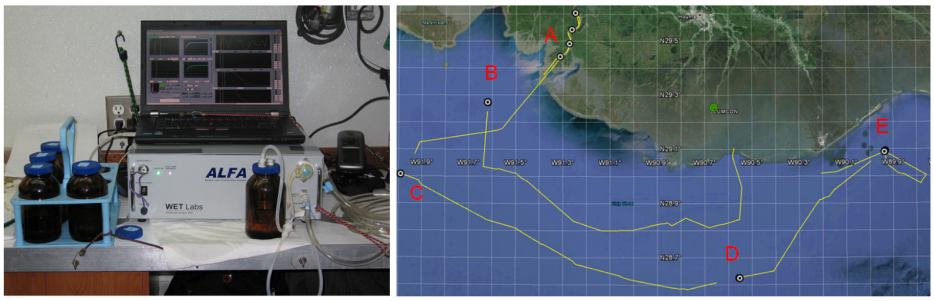

Fig. 1. *Left:* The ALFA instrument setup for the underway flow-through measurements and discrete sample analysis (R/V *Pelican*; Apr. 2012). *Right:* A map of ALFA underway measurements and sampling stations in the Northern Gulf of Mexico in April 2012.

In this article, we present results of the initial field evaluation of the ALFA-405/514 instrument and its analytical capabilities during a research cruise of the R/V *Pelican* in the Northern Gulf of Mexico in April 2012. The new ALFA instrument was used in conjunction with traditional oceanographic instruments (Turner 10AU fluorometer) and analytical techniques (high performance liquid chromatography (HPLC)) to provide additional, often missing information about spatial variability in phytoplankton biomass, photochemical efficiency, community structure, and CDOM abundance across the estuarine-marine gradient in the coastal zone influenced by the Mississippi-Atchafalaya River system. The measurements were conducted in collaboration between the research teams of Columbia University, Texas A&M University (Galveston campus), and WET Labs.

The Mississippi-Atchafalaya River system is the end-point for the largest drainage system in the United States, moving water from parts or all of 31 states [13,14]. While many studies focused on the relationship between phytoplankton biomass and productivity to nutrients in the Northern Gulf of Mexico (e.g., [13–15]), few studies have investigated phytoplankton physiology [16–19] and community composition (e.g., [19–21]). This is partly due to the challenges associated with traditional approaches such as microscopic taxonomy or HPLC, which are very time/labor consuming and require professionally trained specialists. The ALF and other new optical techniques can provide a means for field studies and environmental surveys to improve our understanding of aquatic biogeochemical processes and advance our capacity to monitor state of health of aquatic ecosystems.

2. ALFA measurements

The ALFA-405/514 measurement protocols are similar to those used in the ALF-T instrument [3]. During the in-line underway measurements, the ALFA instrument continuously repeats the basic measurement cycle including:

(1) the broadband (400-800 nm) LSE spectral measurement with the 405 nm excitation,

(2) the broadband (500-800 nm) LSE spectral measurement with the 514 nm excitation,

#214306 - $15.00 USD Received 18 Jun 2014; revised 15 Aug 2014; accepted 15 Aug 2014; published 29 Aug 2014

(3) the pump-during-probe (PDP [1,4,22]) temporal measurement of the LSE induction over 200 μs with the 405 nm excitation,

(4) the PDP temporal measurement of the LSE induction over 200 μs with the 514 nm excitation.

The discrete sample analysis begins with two PDP induction measurements using the 405 and 514 nm excitation, followed by the LSE spectral measurements with the alternate 405 and 514 nm excitation. The spectral integration time is automatically adjusted in 0.1-3 s range to optimize the signal:noise ratio and avoid saturation of the CCD sensor. The PDP induction curves are averaged over the preset number of excitation shots to ensure representative measurements in the sample volume and improve the signal. The gain and input range of the PDP sensor are automatically adjusted to optimize the PDP measurements.

The raw spectra are corrected for the instrument spectral response immediately after the measurements as described in [4] to obtain the instrument-independent spectral data. The real-time SDC analysis of the overlapped spectral bands is incorporated in the ALFA software for assessment of Chl concentration, PBP pigments and CDOM. The intensities of fluorescence bands are normalized to water Raman scattering (WR) to improve the accuracy of fluorescence assessments [1,23,24]. The PY values (i.e., the quantum yield of photochemistry in photosystem II) are also derived in real time from the spectrally corrected PDP induction measurements using a bio-physical model as described in [1,4].

The ALFA measurements described herein were conducted in April 24-30, 2012. The ALFA instrument was installed in the laboratory of the R/V *Pelican* [Fig. 1] and used for analysis of discrete water samples collected at various depths at the stations, and for high-resolution underway flow-through measurements between the sampling stations. A map in Fig. 1 shows locations of the sampling stations (marked with letters) and the transect lines of the underway ALFA measurements between the stations. Overall, 8353 underway measurement cycles were conducted by the ALFA instrument over the total distance of 601.6 km, resulting in the average spatial resolution of 72 m. For the underway operation, the instrument was connected to the shipboard uncontaminated system that provided continuous sampling of sub-surface water at 2.5 m depth. The ALFA was controlled by a notebook computer using software developed under the LabView environment (National Instruments). A compact GPS unit (MAP76Cx, Garmin) with an external marine antenna (Model 010-12017-00, Garmin) was connected to the instrument computer to provide coordinate and time information during the underway ALFA measurements. The PAR sensor, model SQ-110 (Apogee Instruments), was installed on the upper deck and connected to the ALFA instrument to import the PAR data during the ALFA underway measurements.

Examples of the ALFA measurements in diverse water types are shown in Fig. 2, displaying the screenshots of the ALFA user interface during the measurements. The measurement locations are marked with letters A, B, C, and D, respectively, on the map in Fig. 1. The measured LSE spectra with 405 and 514 nm excitation are displayed with blue and green dots in the left and middle panels, respectively; the golden lines represent the SDC best fits based on the linear scaling of the spectral components [1,4]. The apparent changes in intensity of the CDOM and Chl fluorescence (CF) (blue and green bands) vs. WR peak (red) reflect variations in the concentration of these constituents in fresh (A), coastal (B), and offshore (C and D) waters. A substantial variability in phycoerythrin (PE) fluorescence of green-water cyanobacteria (yellow peak at 578 nm) vs. WR is also evident in the LSE spectra measured with 514 nm excitation (middle panels). The PE fluorescence bands of eukaryotic cryptophytes (590 nm) and blue-water cyanobacteria (565 nm) were also detected by the SDC analysis of the green-stimulated LSE spectra measured offshore (panels C_S^{514}, and D_S^{514}). The fluorescence band of phycocyanin present in photosynthetic apparatus of these PBP-containing phytoplankton groups [1,3] can be seen in the green-stimulated spectra at 644 nm (middle column in Fig. 2). Consistently with the earlier observations (e.g., [1,4,11,25,26]), the

#214306 - $15.00 USD Received 18 Jun 2014; revised 15 Aug 2014; accepted 15 Aug 2014; published 29 Aug 2014

spectral overlap of emission bands of various aquatic constituents is evident in a broad spectral range, particularly in the green-stimulated spectra. The real-time SDC analysis is incorporated in the ALFA software to quantify the intensities of spectral bands of the fluorescence constituents and WR scattering [1,4].

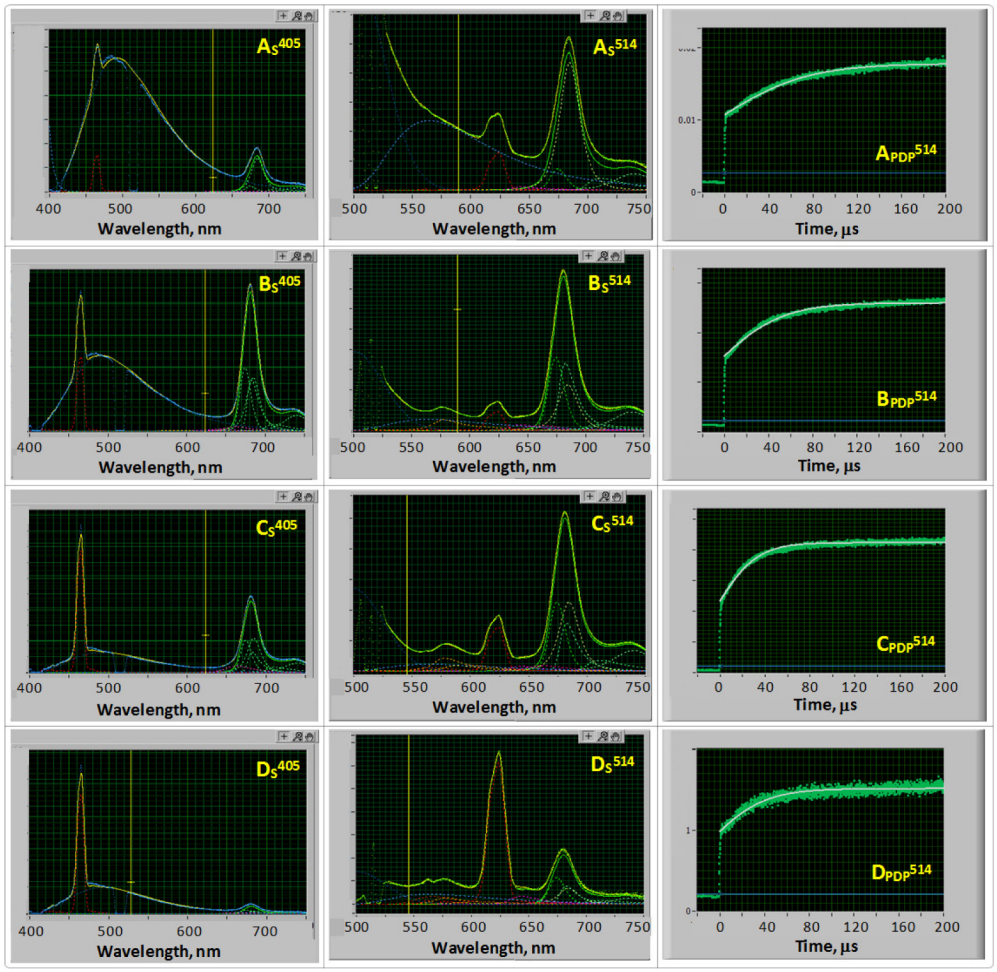

Fig. 2. ALFA measurements using laser excitation at 405 nm (left column) and 514 nm (middle column: LSE spectra; right column: PDP induction). The locations of measurements are marked as A, B, C, and D, respectively, in Fig. 1.

The temporal PDP measurements of the LSE induction in the CF spectral area (~680 nm) using 514 nm excitation are displayed in the right column of Fig. 2. The "0" time marks the beginning of the excitation flash; the blue horizontal line visualizes the intensity of the non-Chl fluorescence background calculated from the SDC analysis of the spectra displayed in the middle column of Fig. 2. This background is subtracted from the LSE induction before best fitting with the biophysical model (white line) to assess the PY value [1,4].

#214306 - $15.00 USD Received 18 Jun 2014; revised 15 Aug 2014; accepted 15 Aug 2014; published 29 Aug 2014

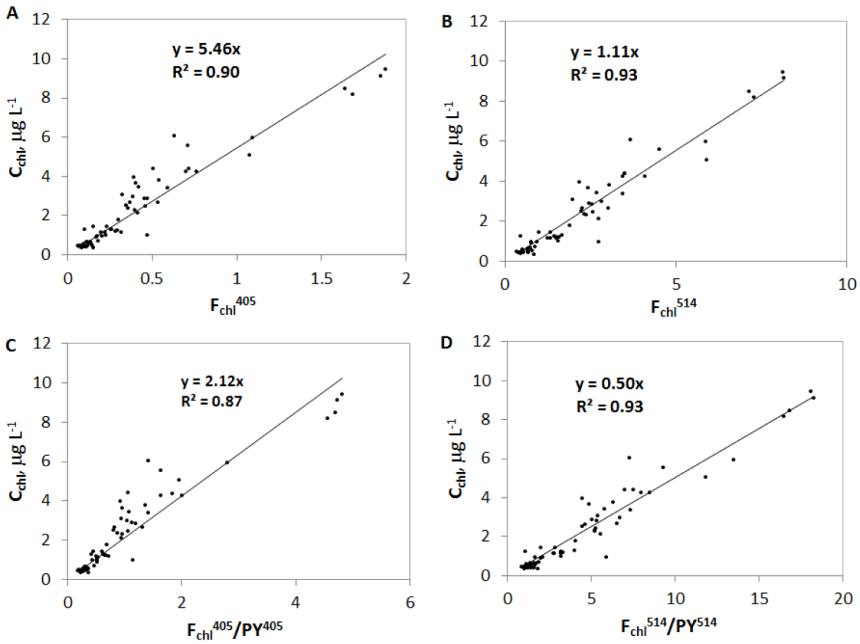

Fig. 3. A,B: The regression relationships between Chl concentration (C_{chl}) in water samples and Chl fluorescence normalized to WR (F_{chl}) measured with 405 and 514 nm excitation. C,D: The regression relationships between C_{chl} in water samples and F_{chl} normalized to phytoplankton photochemical efficiency (PY) measured with 405 and 514 nm excitation (data for the same set of samples as in panels A and B).

3. Fluorescence analysis of Chl concentration and PBP-containing phytoplankton

The results of linear regression between the measurements of Chl concentration (C_{chl}) in pigment extracts [10] and the ALFA measurements of CF normalized to WR (F_{chl} [1,4],) are displayed in Figs. 3(A) and 3(B). The F_{chl}^{405} and F_{chl}^{514} values were calculated by the ALFA software using SDC analysis of the LSE spectra measured with 405 and 514 nm excitation, respectively, in the dark-adapted water samples collected at the locations marked with letters on the map in Fig. 1. The slope value in Fig. 3(A) is close to the magnitudes earlier derived in the estuarine and coastal waters using 405 nm excitation [1,2], but ~2-fold greater than the slope obtained in the California Current waters [4, 11]. The slope value in Fig. 3(B) is also ~2-fold higher than observed in the California Current. We assume that these differences could be caused by the distinct composition of oceanic phytoplankton in the California Current, resulting in their higher CF yield.

Figs. 3(C) and 3(D) show the linear regression relationships between C_{chl} and the fluorescence parameter F_{chl}/PY (i.e., the ratio of F_{chl} and PY values) measured using the 405 and 514 nm excitation, respectively. As shown in [2], the use of the F_{chl}/PY units for assessment of Chl concentration from the daytime underway fluorescence measurements may be beneficial, because it appears to be invariant with regard to the solar-induced non-photochemical quenching (NPQ) that may adversely affect the accuracy of C_{chl} assessments based on the F_{chl} underway measurements. As evident from Figs. 3(C) and 3(D), the F_{chl}/PY values have shown the robust regression relationships with the independent measurements of Chl concentration. The slope value in Fig. 3(C) is close to the slope magnitude measured in the estuarine waters of the Chesapeake and Delaware Bays (1.88 [2];), suggesting that this approach may potentially be used to improve the accuracy of the Chl fluorescence assessment in a broad range of coastal end estuarine water types.

#214306 - $15.00 USD Received 18 Jun 2014; revised 15 Aug 2014; accepted 15 Aug 2014; published 29 Aug 2014

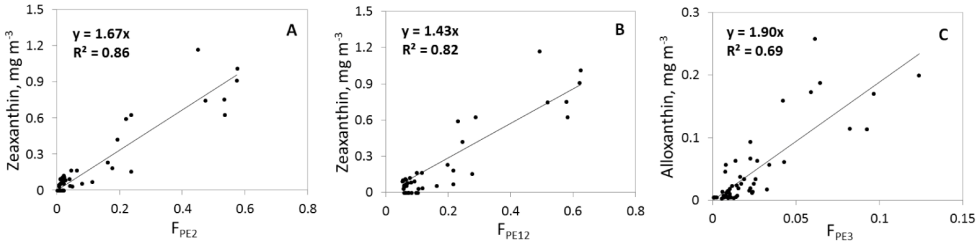

Fig. 4. The regression relationships between the ALFA measurements of (A) PE fluorescence of green-water cyanobacteria, F_{PE2}^{514}, (B) total cyanobacterial PE fluorescence, F_{PE12}^{514}, and (C) cryptophyte-specific PE fluorescence, F_{PE3}^{514}, and HPLC measurements of their respective pigment biomarkers zeaxanthin and alloxanthin. The data for sub-surface layer (0.3-12 m) sampled at stations A-E (Fig. 1) are displayed in panels A,B; panel C shows the data from 0.3 to 19 m layer.

Our recent field measurements in the California Current have demonstrated that the 514 nm laser excitation can be used for assessment of blue-water cyanobacteria and cryptophytes [11], but low concentration of green-water cyanobacteria has not permitted testing the 514 nm excitation for their fluorescence assessment. Fortunately, we found high enough concentration of green-water cyanobacteria in the coastal zone of Northern Gulf of Mexico to conduct the test. Similar to our approach used for blue-water cyanobacteria and cryptophytes [1,11], the test was based on analyzing the relationship between the accessory pigment zeaxanthin and the specific for green-water cyanobacteria PE fluorescence peak at 578 nm [1], normalized to WR scattering (F_{PE2}^{514}).

As shown by earlier studies (e.g., [27,28]), photoacclimation of cyanobacterial photosynthetic apparatus to low-light conditions in deeper water layers may lead to significant increase in the PE cellular quotas with depth. During our recent measurements in the California Current we found that this may result in considerable, up to 10-fold, increase with depth in the cyanobacterial PE fluorescence per unit of their carbon biomass, which complicated fluorescence assessments of cyanobacterial biomass in the euphotic layer [3]. On the other hand, the ALF data has shown strong linear regression relationship between the cyanobacterial PE fluorescence and their biomass in the subsurface water layer above the Chl maximum ($R^2 = 0.95$ vs. 0.42 for the entire euphotic layer), which was used to build the high-resolution surface distribution of *Synechococcus* carbon biomass using the ALF underway PE fluorescence measurements [3].

During our ALFA field measurements in Northern Gulf of Mexico, most of the water samples were collected in the 0.3-12 m subsurface layer above the Chl maximum, and the maximum depth of sampling did not exceed 19 m, which was above or below the shallow Chl maximum, depending on the station location. To evaluate the ALFA potential for assessment of cyanobacterial biomass, we analyzed both the entire data set, and the subset of subsurface (0.3-12 m) ALFA measurements of cyanobacteria-specific PE fluorescence vs. HPLC concentration measurements of accessory carotenoid pigment zeaxanthin.

Although zeaxanthin is often used as a cyanobacterial pigment biomarker (e.g. [29]), it is not 100% specific for cyanobacteria. Photosynthetic apparatus of chlorophytes and eustigmatophytes (non-PBP-containing phytoplankton groups) may also contain zeaxanthin. The potential presence of these two groups in substantial and variable proportion vs. cyanobacteria may result in reduced correlation between the cyanobacteria-specific PE fluorescence and less-specific zeaxanthin. In fact, we obtained quite robust linear regression relationship between the ALFA F_{PE2}^{514} measurements and zeaxanthin concentration in the subsurface water layer (0.3-12 m) above the Chl maximum (Fig. 4(A); $R^2 = 0.86$). This suggests that zeaxanthin was mainly associated with green-water cyanobacteria in the area of study. Indeed, our ALFA underway measurements have shown relatively high concentration of green-water cyanobacteria, and large areas where they comprised a significant fraction of

#214306 - $15.00 USD Received 18 Jun 2014; revised 15 Aug 2014; accepted 15 Aug 2014; published 29 Aug 2014

phytoplankton community (see Section 6). We also obtained reasonably good correlation between F_{PE2}^{514} and zeaxanthin for the entire data set ($R^2 = 0.77$). Consistent with our earlier observations [3], it was reduced vs. the sub-surface data above the Chl maximum, likely due to the gradual photo-acclimative increase in the PE fluorescence:biomass ratio below the Chl maximum. Further, in a parallel study using HPLC to examine pigment composition of water samples and phytoplankton community analysis during the same cruise [19], chlorophytes and eustigmatophytes comprised ≤ 5% of the community.

Interestingly (and in contrast with our observations in the offshore oceanic waters [1,3]), the F_{PE1}^{514} fluorescence (PE peak at 565 nm; normalized to WR) of blue-water cyanobacteria [1], less abundant in the area of study, showed weak correlation with zeaxanthin concentration, which was likely associated with more abundant green-water cyanobacteria. Consistent with such assumption, the regression relationship between zeaxanthin and total cyanobacterial fluorescence $F_{PE12}^{514} = F_{PE1}^{514} + F_{PE2}^{514}$ appeared to be almost as robust for the green-cyanobacteria ($R^2 = 0.82$ for the subsurface (0.3-12 m) samples above Chl maximum; Fig. 4(B)). The ALFA measurements of F_{PE3}^{514} fluorescence of cryptophytes (PE peak at 590 nm; normalized to WR) also indicated their relatively low abundance vs. green-water cyanobacteria (maximal F_{PE3}^{514} ~0.12 vs. 0.56 for F_{PE2}^{514}; Fig. 4). Nonetheless the F_{PE3}^{514} data showed good correlation with HPLC measurements of their specific pigment biomarker, alloxanthin, for the entire set of samples from 0.3 to 19 m (Fig. 4(C); $R^2 = 0.69$). In contrast with cyanobacteria, the subsurface (0.3-12 m) subset of data for cryptophytes did not show higher correlation, suggesting no clear photo-acclimative trends in the F_{PE3} cryptophyte fluorescence.

The robust regression relationships between the group-specific PE fluorescence and concentration of pigment biomarkers associated with the PBP-containing phytoplankton demonstrate that the ALFA spectral measurements of fluorescence stimulated at 514 nm can be used for detection, identification, and quantitative assessments of the PBP-containing cryptophytes and cyanobacteria. These and earlier published data (e.g., [1,3]) suggest that the cryptophyte biomass can be estimated with reasonably good accuracy in the entire euphotic layer. For cyanobacteria, it can be also done in the subsurface layer above the Chl maximum [3]. An important practical application is that the underway fluorescence measurements from various moving platforms (ships, small vessels, autonomous surface vehicles) can be used for real-time high-resolution assessments of horizontal distributions of cyanobacterial biomass along with other key aquatic characteristics (Chl, PY, CDOM, etc.; for example, see [3]). The ALF technique can be also employed for long-term monitoring of cyanobacterial biomass and other relevant characteristics in the surface waters in stationary settings (buoys, platforms, etc.). The methodology of fluorescence assessment of cyanobacterial biomass at the euphotic depths below Chl maximum however needs additional research, involving (and accounting for) the photo-acclimative changes in the cyanobacterial fluorescence:biomass ratio.

The complementary chromatic adaptation (CCA) of cyanobacterial photosynthetic apparatus (e.g., [30]) should be considered in this context among other photo-acclimative mechanisms. A detailed discussion of this biophysical phenomenon is beyond the scope of this publication focused on the field evaluation of the new instrument. To summarize, some (not all (e.g., [31])) cyanobacterial strains may exhibit the CCA that results in altering the relationship between light absorption by the phycourobilin (PUB) and phycoerythrobilin (PEB) chromophore due to the prolonged (~days) effect of change in spectral composition of the ambient light. The CCA does not affect the spectral characteristics of PE fluorescence and, therefore, the accuracy of spectral fluorescence detection and identification of the PBP-containing cyanobacteria (e.g [26].). On the other hand, it may alter the cyanobacterial light absorption in the blue-green spectral range, and, therefore, affect the efficiency of fluorescence excitation with a green laser. The CCA may develop with depth in the stratified euphotic layer because of alteration in the spectral composition of the ambient light field. In particular, it could contribute to the increase with depth in the cyanobacterial PE

#214306 - $15.00 USD Received 18 Jun 2014; revised 15 Aug 2014; accepted 15 Aug 2014; published 29 Aug 2014

fluorescence:biomass ratio (e.g., [3]). The robust regression relationships in Figs. 4(A) and 4(B)) suggest no significant CCA effect in the subsurface water layer (0.3-12 m) in the area of study. The underway ALFA measurements of PE fluorescence are analyzed below in Sections 4 and 6 under this assumption.

4. ALFA underway transect measurements

Fig. 5 shows an example of underway measurements with the ALFA instrument during the outbound ship transient between the sampling stations E and D [Fig. 1]. The dots represent 1626 measurements automatically conducted over a distance of 79.1 km, resulting in spatial resolution of 48.6 m per measurement cycle. The measurements began at 6:54 am (Central Standard Time), and were finished at 13:10 pm the day of April 26, 2012 (right to left on Fig. 5). The ALFA underway measurements have provided quite informative data set for characterization of transition from coastal to offshore marine environment. In particular, the gradual decline in CDOM fluorescence (F_{CDOM}^{514}; Fig. 5(C)) indicated an outbound decrease in the CDOM content. Even stronger, ~8-fold offshore CF reduction was observed along the transect line (F_{chl}^{514}; Fig. 5(A)). Though this decrease was generally consistent with the transition from the high-biomass coastal to low-biomass offshore waters, a potential diel modulation by the solar-induced NPQ might also contribute to the CF transect variability. As discussed in [2], the photoprotective NPQ regulation may affect both CF and PY measurements of sub-surface phytoplankton, which has to be accounted for when interpreting the underway measurements over extended period of time. As evident from Fig. 5(C), the PAR intensity on the water surface increased from 146 μM photons m^{-2} s^{-1} at 6:54 in the morning, when departing station E [Fig. 1], to >2000 μM photons m^{-2} s^{-1} at the end of the transect (station D; Fig. 1). Such significant PAR rise could result in the gradual NPQ development in the subsurface phytoplankton, leading to the NPQ-caused reduction in the PY and CF values [2]. Indeed, the diel increase in PAR along the transect line was accompanied by the gradual, up to 30% decline in PY (PY^{514}; Fig. 5(C)). Assuming that the PY reduction was primarily caused by the NPQ development rather than an offshore decrease in phytoplankton photochemical efficiency, we analyzed the correlation between the PY^{514} and PAR values measured along the transect line. The strong linear regression relationship between these variables (R^2 = 0.83; Fig. 6(A)) appeared to be consistent with such assumption.

We speculate that (i) the solar-induced NPQ was indeed the main cause of the underway PY^{514} variability along this transect line, and (ii) the maximal potential PY values for dark-adapted (PAR = 0) phytoplankton, PY_m, would be relatively high (~0.5) all across the transect line. The latter is consistent with the earlier PY measurements in the nutrient-rich coastal and near-shore waters during the spring bloom in the northern Gulf of Mexico and other areas (e.g., [16–19,32]). The CF and PY decrease with increasing PAR was also apparent in the underway ALFA measurements at other locations during this survey, but the spatial/temporal patterns were more complex. It likely reflected a combined effect of both diel NPQ modulation and spatial variability in CF and PY caused by other natural factors, such as nutrient supply and mixing in the water column.

As shown in [2], the NPQ effect on the accuracy of C_{chl} assessments from the underway fluorescence measurements can be eliminated by using the NPQ-invariant CF:PY ratio, instead of the NPQ-affected CF, to calculate the C_{chl} values. Following this approach, we calculated the C_{chl} transect distributions from the ALFA underway measurements [Fig. 7(A)] using the robust regression relationship $C_{chl} = 0.50\ F_{chl}^{514}/PY^{514}$ obtained for the water samples collected at the stations [Fig. 3(D)]. Examples of C_{chl} transect distribution calculated using the F_{chl}^{514} and PY^{514} underway data (Figs. 5(A) and 5(C), respectively) is shown in Fig. 5(C). Note that it indicates a smaller, ~5-fold offshore decline in Chl concentration vs. up to 8-fold decline in CF [Fig. 5(A)], which was also affected by the gradual diel NPQ development during the outbound transect measurements. Based on these C_{chl} estimates, the

#214306 - $15.00 USD Received 18 Jun 2014; revised 15 Aug 2014; accepted 15 Aug 2014; published 29 Aug 2014

offshore waters in the western part of the transect can be qualified as mesotrophic ($0.1<C_{chl}<1$ μg L^{-1}), while the coastal waters in the eastern part of the transect were rather eutrophic ($C_{chl}>1$ μg L^{-1}). Such relationships have been previously documented in this region (e.g., [18,19]). Assuming that the robust relationship between the PY and PAR [Fig. 6(A)] describing the diel NPQ regulation of PY was applicable to the entire area of our survey, we used the ALFA underway measurements of PY and PAR to calculate the spatial distributions of physiological parameter $PY_m = PY\ (1 - 1.35 \cdot 10^{-4}\ PAR)^{-1}$ that characterized the maximal potential PSII photochemical efficiency of dark-adapted phytoplankton, not affected by the NPQ (see Fig. 7(B)).

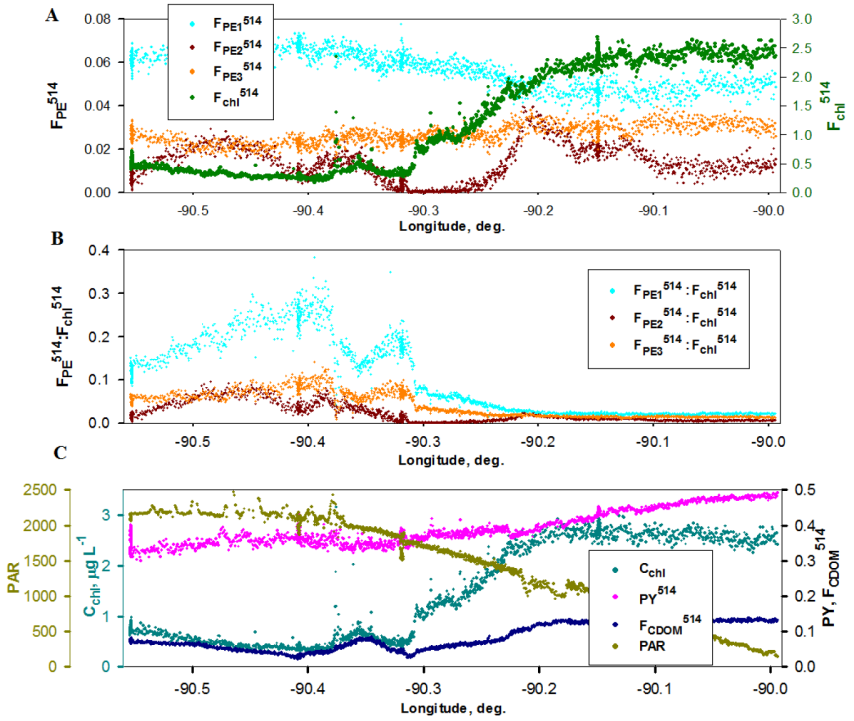

Fig. 5. An example of underway measurements with the ALFA instrument during the outbound ship transient between the sampling stations E and D (Fig. 1).

The ALF underway measurements of pigment fluorescence can also provide important (though not comprehensive) information about the spatial variability in phytoplankton composition [3,8,9]. In particular, the transect distribution of F_{PE1}^{514} fluorescence specific for blue-water cyanobacteria displayed in Figs. 5(A) and 5(B) indicates ~30% increase in their biomass in the offshore portion of the surveyed area. The F_{PE2}^{514} and F_{PE3}^{514} patterns show the opposite trends, with an overall offshore decrease in green-water cyanobacteria and cryptophytes, respectively (the former were not detected at all in the middle of the transect). The contrast between the coastal and offshore portions of the transect is even more apparent in the F_{PE}/F_{chl} patterns [Fig. 5(B)] indicating the substantial offshore increase in relative abundance of the PBP-containing photosynthesizing groups in phytoplankton community [1,3]. The particularly striking, 10-fold increase in the F_{PE1}^{514}:F_{chl} ratio was detected for the blue-water cyanobacteria that have high PUB/PEB ratio, making them better adapted for light harvesting in the offshore blue waters ([1] and references therein). The maximal F_{PE1}^{514}:F_{chl} values ~0.3 suggest that the blue-water cyanobacteria were dominant in the offshore phytoplankton community, comprising up to 80% of total phytoplankton biomass [3]. On the

#214306 - $15.00 USD Received 18 Jun 2014; revised 15 Aug 2014; accepted 15 Aug 2014; published 29 Aug 2014

other hand, the relatively low F_{PE}/F_{chl} magnitudes in coastal waters in the eastern portion of the transect suggests that the elevated Chl concentration observed there [Fig. 5(C)] could be attributed to the increase in biomass of non-PBP-containing eukaryotic phytoplankton.

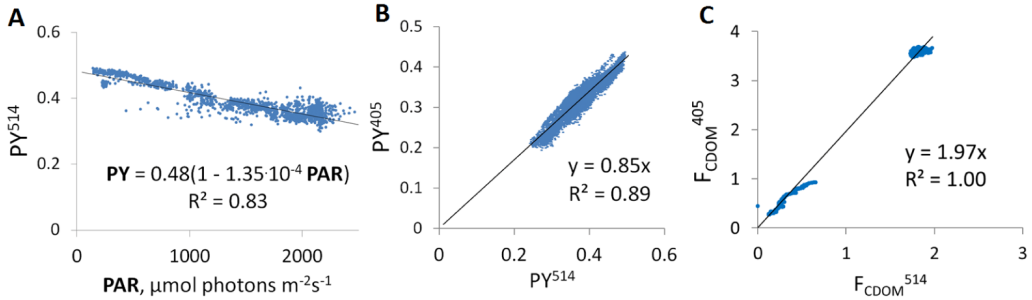

Fig. 6. (A): The regression relationship between the photosynthetically active radiation, PAR, and the ALFA underway measurements of phytoplankton photochemical efficiency, PY^{514}, measured underway between the sampling stations D and E (Fig. 1). (B, C): The regression relationships between the ALFA underway measurements of phytoplankton photochemical efficiency, PY, and CDOM fluorescence normalized to WR scattering, F_{CDOM}, measured with 405 and 514 nm laser excitation. The data for all transects shown in Fig. 1 are displayed.

5. Fluorescence assessments of phytoplankton photochemical efficiency and CDOM using ALFA dual-wavelength excitation

The ALFA field measurements described in this article provided an opportunity to evaluate the analytical capabilities of the ALF instrument configured with a new 514 nm diode laser as source of fluorescence excitation in the diverse water types across the estuarine-marine gradient. As evident from the data displayed in Figs. 3 and 4, the 514 nm laser excitation can serve well for pigment fluorescence assessments of Chl concentration and phytoplankton community structure. An example of transect measurements in Fig. 5 shows that it can also provide reasonably good signal:noise ratio for measuring PY and CDOM fluorescence. In Figs. 6(B) and 6(C) we present the results of correlation analysis of underway measurements of these two parameters along all the transect lines displayed in Fig. 1 in a broad range of water types, including fresh, estuarine, coastal and offshore waters.

The results of measuring PY with 405 and 514 nm excitation in the Northern Gulf of Mexico appeared to be consistent with our measurements in the Ligurian Sea (Mediterranean) [11]: both data sets have shown high correlation ($R^2 = 0.89$ [Fig. 6(B)] vs. 0.98 [11]) between the PY^{514} and PY^{405} values, and very close slope magnitudes (0.85 [Fig. 6(B)] vs. 0.87 [4]). Following the interpretation given in [11], we speculate that the 13-15% higher values of PY^{514} vs. PY^{405} may be caused by the greater photochemical efficiency of cyanobacteria. They comprised significant fraction of phytoplankton community (Fig. 5(B); see also Figs. 7(G) and 7(H) and relevant discussion below), but did not adequately contribute to the bulk PY^{405} measurements since the blue light is low-efficient for excitation of their pigment fluorescence (e.g., [1]).

Similar to the ALF measurements in the Gulf of Mexico area adjacent to the Mississippi River delta [11], our analysis of the underway ALFA measurements in the Northern Gulf of Mexico has revealed a robust linear regression relationship between the F_{CDOM}^{514} and F_{CDOM}^{405} (Fig. 6(C); $R^2 = 1$ vs. 0.95 reported in [1]; the slope value is 1.97 vs. 1.81, respecively). The maximal F_{CDOM} magnitudes were measured in the Atchafalaya River, indicating very high CDOM content. An apparent deviation from the regression trendline for $0.3<F_{CDOM}^{514}<0.8$ measured in coastal waters may suggest some structural changes in CDOM components contributing to the CDOM fluorescence.

#214306 - $15.00 USD Received 18 Jun 2014; revised 15 Aug 2014; accepted 15 Aug 2014; published 29 Aug 2014

6. ALFA underway mapping of fluorescence patterns

The ALFA underway measurements have provided rich and informative high-resolution data to characterize spatial distributions of the key fluorescence characteristics in the Northern Gulf of Mexico during the spring phytoplankton bloom in April, 2012 [Fig. 7]. In this section, we briefly discuss these fluorescence patterns to illustrate the analytical capabilities of the ALF technique. A detailed discussion of the oceanographic features of this survey is beyond the scope of this article, and will be given elsewhere. The maps displayed in Fig. 7 were built using ALFA measurements with 514 nm excitation; some distinct features of the fluorescence patterns are marked as 1-6.

The spatial distribution of Chl concentration [Fig. 7(A)] was calculated using the regression equation $C_{chl} = 0.50\ F_{chl}^{514}/PY^{514}$ derived from analyzing discrete water samples at the stations [Fig. 3D]. The NPQ-invariant F_{chl}/PY parameter was used to eliminate the F_{chl} modulation by the NPQ and improve the accuracy of C_{chl} assessments (section 4 and [2]). A significant range of C_{chl} variability, 0.4-12 μg L^{-1}, was detected across the estuarine-marine gradient surveyed in this area. The offshore and coastal locations of C_{chl} minimum and maximum, respectively, are marked as "4" and "6" in Fig. 7.

Fig. 7(B) shows the spatial distribution of phytoplankton physiological parameter PY_m, the NPQ-corrected phytoplankton photochemical efficiency. It was calculated using the ALFA underway measurements of the actual, potentially affected by the NPQ photochemical efficiency, PY, and PAR as $PY_m = PY\ (1 - 1.35 \cdot 10^{-4}\ PAR)^{-1}$, assuming that the regression relationship in Fig. 6(A) is applicable to the entire surveyed area. Though different phytoplankton groups may have different NPQ mechanisms, the ChemTax analysis of the HPLC pigment measurements at the stations has shown that diatoms were dominant phytoplankton group (accounting for 40-80% phytoplankton biomass) in the area of study [19], despite the structural variability among other, subdominant phytoplankton groups. Since the ALFA fluorescence measurements reflect the bulk properties of phytoplankton community, the PY values and NPQ mechanisms involved were therefore mainly determined by the diatoms. This justifies our assumption regarding the applicability of the regression equation for the NPQ correction of the PY measurements. The PY values were derived from the ALFA fluorescence induction measurements corrected for the non-Chl spectral background [1,4], particularly significant in high-CDOM fresh and estuarine waters [Fig. 2A].

The PY_m values also exhibited substantial variability across the area, 0.3-0.65. The highest values, PY_m^{514}~0.6-0.65, were found in the estuarine waters adjacent to the mouth of the Atchafalaya River. These values are close to the maximal photochemical efficiency, 0.65, measured using single-turnover technique for phytoplankton grown in the optimized laboratory conditions (e.g., [33]). It can be rarely observed in the field (e.g., [34]), which is consistent with earlier observations of high photochemical efficiency of healthy phytoplankton in the nutrient-rich estuarine waters in the Gulf of Mexico [16,17]. In contrast, the lowest PY_m magnitudes, indicating low phytoplankton photochemical efficiency, were found offshore ("5" in Fig. 7), where the reduced Chl concentration [Fig. 7(A)], low CDOM content [Fig. 7(C)], and high fraction of green-water cyanobacteria in phytoplankton population [Fig. 7(H)] were also detected.

The CDOM fluorescence distribution [Fig. 7(C)] also varied in a broad range, showing two distinct areas of very high CDOM content in the Atchafalaya River and its estuary (F_{CDOM}^{514} ~2; see also Fig. 6(C)), and more moderate, "coastal" values $0.15 < F_{CDOM}^{514} < 0.7$. Fig. 7(C) clearly shows the transition from the CDOM-rich freshwater/estuarine/coastal waters ("1", "2", and "3" in Fig. 7) to the relatively low-CDOM marine environments ("4", "5", and "6" in Fig. 7). The CDOM patterns appeared to be consistent with spatial distribution of seasurface salinity (not shown).

#214306 - $15.00 USD Received 18 Jun 2014; revised 15 Aug 2014; accepted 15 Aug 2014; published 29 Aug 2014

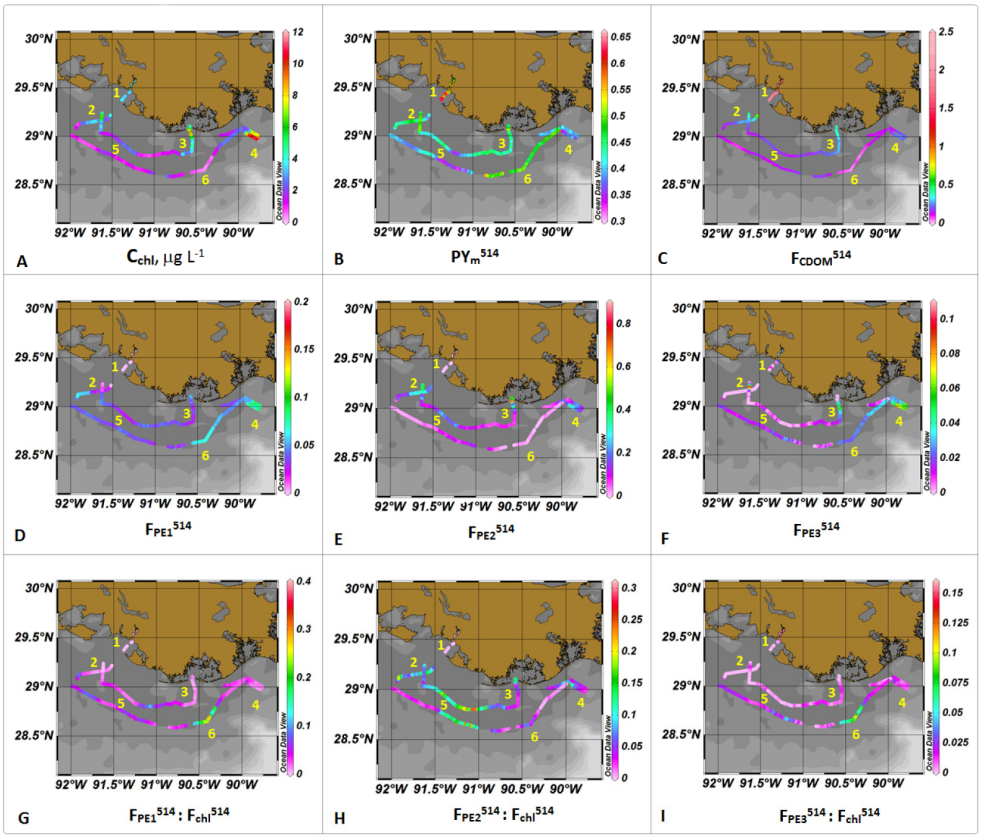

Fig. 7. Spatial distributions of the key fluorescence characteristics in the Northern Gulf of Mexico during the spring phytoplankton bloom in April, 2012 built using the ALFA underway measurements [Fig. 1] with 514 nm excitation.

The fluorescence patterns of the PBP-containing phytoplankton groups [Fig. 7(D) - 7(I)] appeared to be more complex, reflecting both overall changes in phytoplankton biomass across the estuarine-marine gradient and structural changes within the phytoplankton population. Consistent with other ALF measurements in the Gulf of Mexico (and in contrast to our measurements in the oceanic waters ([1,3]), the green-water cyanobacteria appeared to be most abundant among the PBP-containing phytoplankton groups (F_{PE2}^{514} up to 0.8 ("3" in Fig. 7(E)]), and showed spatial patterns similar to the distributions of C_{chl} and F_{CDOM} [Figs. 7(A) and 7(C)]. They seemed to be better adapted to the specific bio-environmental conditions of the Gulf of Mexico. The green-water cyanobacteria comprised significant, dominant at some locations fraction of the phytoplankton population, mainly in the central and western offshore areas ("2" and "5" in Fig. 7(H); and patches "3", "4"). The F_{PE2}/F_{chl} values reaching 0.2-0.3 at "5" suggest that they might comprise up to 80% of total phytoplankton biomass in this offshore, low-productive [Figs. 7(A) and 7(B)] area.

The blue –water cyanobacteria were generally less abundant ($F_{PE1}^{514} < 0.1$), showing their slightly elevated biomass mainly in the low-CDOM waters ("4"-"6", "2" in Fig. 7(D)). Despite their relatively low concentration, they appeared dominant in the phytoplankton community in the low-CDOM [Fig. 7(C)] and low-Chl [Fig. 7(A)] offshore waters ("6" in Fig. 7). In contrast with our observations in oceanic environments and Delaware Bay (e.g [1,8,9], the PBP-containing eukaryotic cryptophytes were detected at relatively low concentrations (F_{PE3}<0.06 in Fig. 7(F)). Nonetheless, they comprised (along with dominant

#214306 - $15.00 USD Received 18 Jun 2014; revised 15 Aug 2014; accepted 15 Aug 2014; published 29 Aug 2014

blue-water cyanobacteria [Fig. 7(G)]) a substantial component of phytoplankton population in the low-Chl, low-CDOM blue-water area "6" [Fig. 7(I)].

7. Conclusions

The new ALFA instrument was used for the underway shipboard measurements and discrete sample analysis to survey phytoplankton and CDOM across the estuarine-marine gradient in the Northern Gulf of Mexico. The total length of the measurement transect lines was 601.6 km; 8353 underway measurement cycles were conducted, resulting in the average spatial resolution of 72 m per cycle. The real-time shipboard fluorescence measurements of the water samples collected at the stations have shown the robust regression relationships with the independent measurements of pigment concentrations that were used for instrument calibration and validation. In particular, the NPQ-invariant ratio of regular and variable Chl fluorescence, $F_{chl} \cdot PY^{-1}$, was used to build the synoptic-scale map of Chl concentration in the area of survey. The robust linear regression relationship between the phytoplankton photochemical efficiency, PY, and photosynthetically active radiation, PAR, was derived from the transect data. It was used to correct the underway PY measurements for the solar-induced NPQ to assess the spatial patterns of the maximal phytoplankton photochemical efficiency, PY_m. The comparative analysis of fluorescence measurements with excitation at 514 nm vs. 405 nm employed in the earlier instrument configurations suggests that the former can be used for fluorescence characterization of the CDOM-rich fresh, estuarine, and coastal aquatic environments. This justifies the development of compact and affordable, yet informative single-laser fluorometers for fluorescence analysis of natural aquatic environments.

Appendix

Table 1. Abbreviations used in text.

Abbreviation	Term
ALF	Advanced Laser Fluorometry/Fluorometer
ALFA	Aquatic Laser Fluorescence Analyzer
CCD	Charge-coupling device
CDOM	Chromophoric dissolved organic matter (substance)
Chl	Chlorophyll a (pigment)
C_{chl}	Chl *a* concentration, μg L^{-1}
CF	Chlorophyll fluorescence
F_{CDOM}	CDOM fluorescence intensity normalized to WR intensity
F_{chl}	CF intensity normalized to WR intensity
F_{PE1}	PE fluorescence of blue-water cyanobacteria (peak at 565 nm) normalized to WR
F_{PE2}	PE fluorescence of green-water cyanobacteria (peak at 578 nm) normalized to WR
F_{PE3}	PE fluorescence of cryptophytes (peak at 590 nm) normalized to WR
HPLC	High performance liquid chromatography
LSE	Laser-stimulated emission
NPQ	Non-photochemical quenching
PAR	Photosynthetically active radiation
PBP	Phycobiliprotein (pigments)
PDP	Pump-during-probe (measurement protocol)
PE	Phycoerythrin (pigment)
PEB	Phycoerythrobilin (chromophore)
PUB	Phycourobilin (chromophore)
PY	Photochemical efficiency of phytoplankton photosystem II
PY_m	Maximal PY magnitude in the absence of NPQ
R^2	Coefficient of determination
SDC	Spectral deconvolution (method, technique)
WR	Water Raman scattering
WET Labs	Western Environmental Technologies, Inc.

#214306 - $15.00 USD Received 18 Jun 2014; revised 15 Aug 2014; accepted 15 Aug 2014; published 29 Aug 2014

Acknowledgments

We thank engineers and technical staff of WET Labs, who participated in the ALFA development, tests, and preparation for the field measurements, and the scientific party and the crew of the R/V *Pelican* for all their help. This work was supported by the National Oceanographic Partnership Programs (award number: N000141010205; administrated by the Office of Naval Research), and National Oceanic and Atmospheric Administration (Grant number: NA09N0S4780208); it will be contribution no. 193 of the CSCOR NGOMEX Project.

#214306 - $15.00 USD Received 18 Jun 2014; revised 15 Aug 2014; accepted 15 Aug 2014; published 29 Aug 2014